

# REPORT DOCUMENTATION PAGE

Form Approved  
OMB NO. 0704-0188

Public Reporting burden for this collection of information is estimated to average 1 hour per response, including the time for reviewing instructions, searching existing data sources, gathering and maintaining the data needed, and completing and reviewing the collection of information. Send comment regarding this burden estimates or any other aspect of this collection of information, including suggestions for reducing this burden, to Washington Headquarters Services, Directorate for Information Operations and Reports, 1215 Jefferson Davis Highway, Suite 1204, Arlington, VA 22202-4302, and to the Office of Management and Budget, Paperwork Reduction Project (0704-0188), Washington, DC 20503.

1. AGENCY USE ONLY (Leave Blank)

2. REPORT DATE  
6/12/2006

3. REPORT TYPE AND DATES COVERED  
Reprint

4. TITLE AND SUBTITLE  
Time-dependent stochastic inversion in acoustic travel-time tomography of the atmosphere

5. FUNDING NUMBERS  
DAAD19-03-1-0104

6. AUTHOR(S)  
S.N. Vecherin, V.E. Ostashev, G.H. Goedecke, D.K. Wilson, and A.G. Voronovich,

7. PERFORMING ORGANIZATION NAME(S) AND ADDRESS(ES)  
Physics Department, New Mexico State University,  
Box 30001, Dept. 3D, Las Cruces, NM 88003

8. PERFORMING ORGANIZATION  
REPORT NUMBER

9. SPONSORING / MONITORING AGENCY NAME(S) AND ADDRESS(ES)  
U. S. Army Research Office  
P.O. Box 12211  
Research Triangle Park, NC 27709-2211

10. SPONSORING / MONITORING  
AGENCY REPORT NUMBER  
45258.12-EV-HSI

11. SUPPLEMENTARY NOTES  
The views, opinions and/or findings contained in this report are those of the author(s) and should not be construed as an official Department of the Army position, policy or decision, unless so designated by other documentation.

12 a. DISTRIBUTION / AVAILABILITY STATEMENT  
Approved for public release; distribution unlimited.

12 b. DISTRIBUTION CODE

13. ABSTRACT (Maximum 200 words)  
See the reprint attached.

14. SUBJECT TERMS

15. NUMBER OF PAGES  
10

16. PRICE CODE

17. SECURITY CLASSIFICATION  
OR REPORT  
**UNCLASSIFIED**

18. SECURITY CLASSIFICATION  
ON THIS PAGE  
**UNCLASSIFIED**

19. SECURITY CLASSIFICATION  
OF ABSTRACT  
**UNCLASSIFIED**

20. LIMITATION OF ABSTRACT  
**UL**

# Time-dependent stochastic inversion in acoustic travel-time tomography of the atmosphere

Sergey N. Vecherin

*Department of Physics, New Mexico State University, Las Cruces, New Mexico 88003*

Vladimir E. Ostashev

*NOAA/Earth System Research Laboratory, Boulder, Colorado 80305 and Department of Physics, New Mexico State University, Las Cruces, New Mexico 88003*

George H. Goedecke

*Department of Physics, New Mexico State University, Las Cruces, New Mexico 88003*

D. Keith Wilson

*U.S. Army Engineer Research and Development Center, Hanover, New Hampshire 03755*

Alexander G. Voronovich

*NOAA/Earth System Research Laboratory, Boulder, Colorado 80305*

(Received 4 August 2005; revised 3 February 2006; accepted 7 February 2006)

Stochastic inversion is a well known technique for the solution of inverse problems in tomography. It employs the idea that the propagation medium may be represented as random with a known spatial covariance function. In this paper, a generalization of the stochastic inverse for acoustic travel-time tomography of the atmosphere is developed. The atmospheric inhomogeneities are considered to be random, not only in space but also in time. This allows one to incorporate tomographic data (travel times) obtained at different times to estimate the state of the propagation medium at any given time, by using spatial-temporal covariance functions of atmospheric turbulence. This increases the amount of data without increasing the number of sources and/or receivers. A numerical simulation for two-dimensional travel-time acoustic tomography of the atmosphere is performed in which travel times between sources to receivers are calculated, given the temperature and wind velocity fields. These travel times are used as data for reconstructing the original fields using both the ordinary stochastic inversion and the proposed time-dependent stochastic inversion algorithms. The time-dependent stochastic inversion produces a good match to the specified temperature and wind velocity fields, with average errors about half those of the ordinary stochastic inverse. © 2006 Acoustical Society of America. [DOI: 10.1121/1.2180535]

PACS number(s): 43.20.Dk, 43.28.We, 43.28.Vd [AIT]

Pages: 2579–2588

## I. INTRODUCTION

Acoustic tomography is widely used in physics, technology, and medicine for the remote sensing of inhomogeneous media. When applied to the atmosphere, acoustic tomography allows one to estimate (reconstruct) temperature and wind velocity within a tomographic volume or area.<sup>1–4</sup> The practical realization of acoustic tomography in an atmospheric boundary layer was reported in Refs. 5–10. In these tomography experiments, the sources and receivers of sound were located on masts several meters above the ground along the perimeter of a tomographic area that was a square or rectangular with side lengths of several hundred meters. The sound travel times between all pairs of sources and receivers were measured and used as input data for inverse algorithms to estimate temperature and wind velocity fields within a horizontal slice. This kind of tomography is called travel-time tomography. The inverse algorithms used were the stochastic inversion (SI) approach<sup>5</sup> and the simultaneous iterative reconstruction technique.<sup>6–10</sup> In the present paper, a generalization of the SI approach in travel-time acoustic to-

mography of the atmosphere is developed that allows one to effectively increase the number of data without increasing the number of sources and receivers.

The idea of travel-time acoustic tomography of the atmosphere is based on the fact that the time required for sound to propagate through a certain volume depends on the adiabatic sound speed (and hence on temperature) and wind velocity within that volume. More specifically, the travel time  $t_i^{\text{tr}}$  of the sound impulse propagation along the  $i$ th ray can be expressed as the following integral along the path  $L_i$  of this ray (e.g., Ref. 11):

$$t_i^{\text{tr}} = \int_{L_i} \frac{dl}{u_g(\mathbf{R})}. \quad (1)$$

Here,  $u_g(\mathbf{R})$  is the group velocity of a sound impulse,  $\mathbf{R}$  is the position vector in three dimensions, and  $i=1, 2, \dots, I$ , where  $I$  is the number of ray paths of sound impulses simultaneously propagating through this volume from sources to receivers. It can be shown<sup>11</sup> that, in the presence of wind, the  $u_g$  can be expressed as  $u_g = [c_L^2(\mathbf{R}) + V^2(\mathbf{R}) + 2c_L(\mathbf{R})\mathbf{n}_i(\mathbf{R}) \cdot \mathbf{V}(\mathbf{R})]^{1/2}$ . Here  $\mathbf{n}_i$  is the unit vector normal to

the wave front of a sound wave,  $\mathbf{V}$  is the vector of wind velocity, and  $c_L$  is the Laplace adiabatic sound speed that relates to the acoustic virtual temperature  $T_{av}$  by

$$c_L^2 = \gamma R_a T_{av}, \quad (2)$$

where  $\gamma \approx 1.41$  is the ratio of the specific heats and  $R_a$  is the universal gas constant for dry air. It is necessary to take into account the specific humidity of the air  $q$  to obtain the values of the actual thermodynamic temperature  $T_{th}$  from the acoustic virtual temperature by using the following relationship:<sup>11</sup>  $T_{av} \cong T_{th}(1 + 0.511q)$ . Note that the acoustic virtual temperature differs from the virtual temperature used by atmospheric scientists. When deriving Eq. (1), it is assumed that  $u_g$  does not depend on time during the propagation of sound impulses. Since in the atmosphere  $c_L \gg |\mathbf{V}|$ , this assumption is valid for tomographic arrays of order of several hundred meters considered in Refs. 5–10 and in Sec. IV. The goal of acoustic travel-time tomography is to estimate the fields  $T_{av}(\mathbf{R})$  and  $\mathbf{V}(\mathbf{R})$  within a tomographic volume, given the travel times  $t_i^t$  and the locations of sources and receivers.

There are different techniques available to solve this problem. Many of them pursue the goal of finding a solution that, after substitution back into Eq. (1), yields travel times as close to the measured ones as possible. These methods are quite reliable and accurate if there are more data points (e.g., travel times) than unknown model values (e.g., total number of points at which the fields are to be reconstructed). However, this condition does not hold for atmospheric tomography unless the reconstruction is performed with low resolution.<sup>2,6–10,12,13</sup> In the opposite case, when the number of unknowns is greater than the number of available data points, such techniques cannot provide a unique solution, and some additional restrictions must be imposed on the sought fields. Since it is unknown in advance whether the actual fields being estimated obey such restrictions, these techniques may yield a spurious solution that perfectly matches the data but has little to do with the real fields.

In contrast, the SI approach is based on the idea that, using the available data, one seeks fields that have the minimum average deviation from the real ones. This approach also requires additional information about the sought fields, namely, the sought fields are treated as random ones with known spatial covariance functions.<sup>1,3,5,14</sup> Although the actual covariance functions in the turbulent atmosphere are not exactly known, they can be approximated by those corresponding to the von Kármán or Gaussian spectra of turbulence.<sup>11,15,16</sup> Note that other techniques that partition the fields into constant-valued grid cells implicitly assume step-like covariance functions, such that the field values are perfectly correlated within a grid cell and completely uncorrelated outside. Such functions are much less plausible than those used in the SI approach. The applicability and advantages of the SI approach in travel-time tomography of the atmosphere with high resolution are demonstrated in Refs. 3 and 5. A disadvantage of SI is that it does not use the fact that the sought fields are correlated not only in space but also in time.

In this paper, a generalization of the SI approach for acoustic travel-time tomography of the atmosphere is developed that allows one to use the data obtained at different times to reconstruct the temperature and wind velocity fields within a tomographic volume at any particular time, by using spatial-temporal covariance functions of these fields. This generalization is called time-dependent stochastic inversion (TDSI).

The general idea of using spatial-temporal covariance functions in SI is known in the literature. For example, it has been successfully used in satellite altimetry of the ocean surface, e.g., Refs. 17 and 18. In altimetry, the deviations of the ocean surface height from its average level are known at certain times and spatial points (along the satellite tracks). The problem is to estimate these deviations at other points (in space and time). Thus, this problem can be formulated as the space-time interpolation problem. There are many different techniques to interpolate the data. However, SI interpolates them in such a way that the covariance of the resulting fields holds true. The application of SI for these purposes was proposed in Ref. 19.

In contrast to satellite altimetry, travel-time tomography cannot be formulated as an interpolation problem, since the fields that are subject to estimation are unknown everywhere. Therefore, the mathematical formalism of TDSI in acoustic travel-time tomography of the atmosphere differs from that in altimetry. In the present paper, this mathematical formalism is developed. To verify that the TDSI approach improves the quality of the reconstruction, a numerical experiment was carried out for two-dimensional (2-D) travel-time acoustic tomography of a horizontal atmospheric layer.

The paper is organized as follows. In Sec. II, a general theory of 2-D TDSI is developed and a formula for the optimal stochastic inversion matrix is derived. Calculations of the covariance matrices that appear in the inversion matrix are presented in Sec. III. In Sec. IV, the numerical experiment of 2-D travel-time acoustic tomography of the atmosphere is described. Some aspects of the SI and TDSI algorithms are discussed in Sec. V. The conclusions are presented in Sec. VI.

## II. THEORY

In this section, the theory of 2-D TDSI is developed. There are three steps that precede this development. First, it is taken into account that  $T_{av}$  and  $\mathbf{V}$  depend not only on the spatial coordinates but also on time  $t$ . Therefore,  $t_i^t$  depends on time  $t$  as well. Second, Eq. (1) is linearized due to specific conditions in the atmosphere, and, with the same degree of accuracy, the travel paths  $L_i$  are approximated by straight lines. Third, it is shown how to reconstruct the spatial mean values of the temperature and wind velocity fields within a tomographic area with the help of the conventional least square estimation. Finally, the problem for the TDSI approach in the reconstruction of temperature and wind velocity fluctuations is stated and a general solution of this problem is obtained.

## A. Linearization

Let  $\tilde{u}(\mathbf{r}, t)$  and  $\tilde{v}(\mathbf{r}, t)$  be  $x$  and  $y$  components of the two-dimensional vector of wind velocity  $\mathbf{V}$ :

$$\mathbf{V}(\mathbf{r}, t) = \tilde{u}(\mathbf{r}, t)\mathbf{e}_x + \tilde{v}(\mathbf{r}, t)\mathbf{e}_y. \quad (3)$$

Here  $t$  is time, a 2-D vector  $\mathbf{r}$  specifies a spatial point within a tomographic area with the Cartesian coordinates  $(x, y)$ , and  $\mathbf{e}_x$  and  $\mathbf{e}_y$  are the unit vectors along the  $x$  and  $y$  axes, respectively. The adiabatic sound speed  $c_L$ , temperature  $T_{av}$ , and wind velocity fields within a tomographic area at time  $t$  can be represented as sums of their spatial average values  $c_0(t)$ ,  $T_0(t)$ ,  $u_0(t)$ , and  $v_0(t)$  and their fluctuations  $c(\mathbf{r}, t)$ ,  $T(\mathbf{r}, t)$ ,  $u(\mathbf{r}, t)$ , and  $v(\mathbf{r}, t)$ :

$$c_L(\mathbf{r}, t) = c_0(t) + c(\mathbf{r}, t), \quad T_{av}(\mathbf{r}, t) = T_0(t) + T(\mathbf{r}, t), \quad (4)$$

$$\tilde{u}(\mathbf{r}, t) = u_0(t) + u(\mathbf{r}, t), \quad \tilde{v}(\mathbf{r}, t) = v_0(t) + v(\mathbf{r}, t).$$

Since in the atmosphere the absolute values of the adiabatic sound speed fluctuations and the wind components are much smaller than the spatial average value of  $c_0$ , Eq. (1) can be linearized to the first order of these fluctuations<sup>2</sup> and the travel paths of sound can be approximated by straight lines:<sup>5,11</sup>

$$t_i^{tr}(t) = \varepsilon_i(t) + \frac{L_i}{c_0(t)} \left( 1 - \frac{u_0(t)\cos\varphi_i + v_0(t)\sin\varphi_i}{c_0(t)} \right) - \frac{1}{c_0^2(t)} \int_{L_i} dl \left( \frac{c_0(t)}{2T_0(t)} T(\mathbf{r}, t) + u(\mathbf{r}, t)\cos\varphi_i + v(\mathbf{r}, t)\sin\varphi_i \right), \quad (5)$$

where  $i=1, 2, \dots, I$  denotes the ray's path number,  $I$  is the total number of travel paths,  $L_i$  is the length of the  $i$ th ray path,  $\mathbf{r} \in L_i$ , and  $\varphi_i$  is the angle of the  $i$ th ray relative to the positive direction of the  $x$  axis. Note that the noise  $\varepsilon_i$  in the  $i$ th measured travel time was added to the right-hand side of Eq. (5). Furthermore, when deriving this equation the following relationship between the fluctuations of temperature and adiabatic sound speed was used:  $c(\mathbf{r}, t) = [c_0(t)/2T_0(t)]T(\mathbf{r}, t)$ . This relationship follows from Eqs. (4) and (2), with accuracy up to the first order of these fluctuations. The inverse problem, which is studied in this paper, is to reconstruct  $c_0$ ,  $T_0$ ,  $T$ ,  $u$ , and  $v$ , given  $t_i^{tr}$ ,  $L_i$ , and  $\varphi_i$ .

## B. Reconstruction of mean fields

The mean values  $T_0$ ,  $u_0$ , and  $v_0$  within a tomographic area at any time can be reconstructed with the help of the least square estimation by using the travel times obtained at the same moment of time. For this purpose one should set the fluctuating parts of these fields to zero, so that the integral in Eq. (5) vanishes. Then Eq. (5) can be rewritten in matrix notation:

$$\mathbf{G}\mathbf{f} = \mathbf{b}, \quad (6)$$

where the elements of the column vector  $\mathbf{b}$  are known and given by  $b_i = t_i^{tr}(t)/L_i$ , the unknown column vector  $\mathbf{f}$  has

three elements,  $f_1 = 1/c_0(t)$ ,  $f_2 = u_0(t)/c_0^2(t)$ ,  $f_3 = v_0(t)/c_0^2(t)$ , and the matrix  $\mathbf{G}$  is given by

$$\mathbf{G} = \begin{bmatrix} 1 & -\cos\varphi_1 & -\sin\varphi_1 \\ \vdots & \ddots & \vdots \\ 1 & -\cos\varphi_I & -\sin\varphi_I \end{bmatrix}. \quad (7)$$

Then, using the  $I$  elements of the vector  $\mathbf{b}$  ( $I$  is assumed to be greater than 3), one should solve the overdetermined problem for the three unknowns (the elements of the vector  $\mathbf{f}$ ) using the least square estimation:

$$\mathbf{f} = (\mathbf{G}^T\mathbf{G})^{-1}\mathbf{G}^T\mathbf{b}, \quad (8)$$

extract from them the values of  $c_0$ ,  $u_0$ , and  $v_0$ , and calculate  $T_0$  using Eq. (2).

## C. Time-dependent stochastic inversion

Once the spatial mean values of temperature, adiabatic sound speed, and wind velocity fields within a tomographic area are known, it is worthwhile to introduce the column vector of data  $\mathbf{d}(t)$  obtained at time  $t$  with elements

$$d_i(t) = L_i[c_0(t) - u_0(t)\cos\varphi_i - v_0(t)\sin\varphi_i] - c_0^2(t)t_i^{tr}(t) + \xi_i(t), \quad (9)$$

where noise  $\xi_i(t)$  includes the errors of travel time measurements  $\varepsilon_i(t)$  and errors in the estimation of  $T_0$ ,  $c_0$ ,  $u_0$ , and  $v_0$ . Using Eq. (5), this data vector can be expressed as  $\mathbf{d}(t) = \mathbf{d}_0(t) + \boldsymbol{\xi}(t)$ , where the elements of the noise-free data column vector  $\mathbf{d}_0(t)$  are given by

$$d_{0i}(t) = \int_{L_i} dl \left( \frac{c_0(t)}{2T_0(t)} T(\mathbf{r}, t) + u(\mathbf{r}, t)\cos\varphi_i + v(\mathbf{r}, t)\sin\varphi_i \right). \quad (10)$$

The problem now is to reconstruct the fields of fluctuations  $T(\mathbf{r}, t_0)$ ,  $u(\mathbf{r}, t_0)$ , and  $v(\mathbf{r}, t_0)$  at any chosen time  $t_0$ . Thus, the column vector of models at this time moment  $t_0$  is given by

$$\mathbf{m}(t_0) = [T(\mathbf{r}_1, t_0); \dots; T(\mathbf{r}_J, t_0); u(\mathbf{r}_1, t_0); \dots; u(\mathbf{r}_J, t_0); v(\mathbf{r}_1, t_0); \dots; v(\mathbf{r}_J, t_0)], \quad (11)$$

where  $J$  is the number of spatial points within the tomographic area at which the fields are being reconstructed; here and in what follows, the semicolon between elements denotes that these elements are arranged in a column.

Let us assume that one can collect data  $(N+1)$  times during the time  $N\tau$  by performing sound scans of the tomographic area and forming the vector  $\mathbf{d}$  at each scan. Suppose that the last scan was performed at the time  $t$ , which can be earlier, equal to, or later than the time  $t_0$  at which one tries to reconstruct the models. In this paper it is assumed that these scans are performed at equal time intervals  $\tau$ , although such an assumption is not necessary. The temperature and wind velocity fields in this tomographic area are changing with time, which yields different data vectors at each scan. In this case, at the time  $t$  there will be data available from  $(N+1)$  scans. That is, at the moment  $t$  one can form the vector  $\mathbf{d}$  of all available data:

$$\mathbf{d} = [\mathbf{d}(t - N\tau); \mathbf{d}(t - N\tau + \tau); \dots; \mathbf{d}(t)]. \quad (12)$$

Here  $\mathbf{d}$  is a column vector containing the  $(N+1)$  column-vectors  $\mathbf{d}(t-n\tau)$ , each of length  $I$ , where  $n=0,1,\dots,N$ . Therefore, the total length of the data vector  $\mathbf{d}$  is  $(N+1)I$ .

### 1. Problem statement

Using the data vector  $\mathbf{d}$  given by Eq. (12), it is necessary to find a linear estimation  $\hat{\mathbf{m}}(t_0)$  of unknown models  $\mathbf{m}(t_0)$  at time  $t_0$ . The case  $t_0 > t$  corresponds to advanced estimation; the case  $t_0 < t$  corresponds to posterior estimation; and  $t_0 = t$  corresponds to a real time reconstruction. In all these cases, one can use available data obtained from all scans to estimate the unknown fields. If one uses only the data obtained at moment  $t_0$  to estimate the models  $\mathbf{m}(t_0)$  at the same moment, that would correspond to standard SI in atmospheric travel-time tomography.<sup>5</sup>

In TDSI, the estimation of the unknown fields is sought in the same form as in standard SI:

$$\hat{\mathbf{m}}(t_0) = \mathbf{A}\mathbf{d}, \quad (13)$$

where unknown elements  $a_{jk}$  of matrix  $\mathbf{A}$  must be determined. Here  $j=1,2,\dots,3J$ , where  $3J$  is the length of models, and  $k=1,2,\dots,(N+1)I$ . We now introduce the column vector of discrepancy  $\epsilon$  between the true and reconstructed fields at time  $t_0$ :

$$\epsilon_j = \hat{m}_j(t_0) - m_j(t_0). \quad (14)$$

To find the elements  $a_{jk}$ , let us require that they give the minimum of the elements of the mean square errors vector  $\langle \epsilon^2 \rangle$ :

$$\langle \epsilon_j^2 \rangle \mapsto \min_{\{a_{jk}\}} \langle \epsilon_j^2 \rangle, \quad (15)$$

where parentheses  $\langle \cdot \rangle$  denote the mathematical expectation. These mean square errors are the diagonal elements of the error covariance matrix  $\mathbf{R}_{\epsilon\epsilon}$ :

$$\mathbf{R}_{\epsilon\epsilon} \equiv \langle \epsilon\epsilon^T \rangle, \quad (16)$$

where  $\epsilon$  is the column vector of discrepancy given by (14).

### 2. Solution

The matrix  $\mathbf{A}$  that solves the problem stated above is given by the same formula as for ordinary SI, since the derivation of this formula does not depend on a particular structure of the models  $\mathbf{m}$  and data  $\mathbf{d}$  (see Appendix A):

$$\mathbf{A} = \mathbf{R}_{\mathbf{m}\mathbf{d}}\mathbf{R}_{\mathbf{d}\mathbf{d}}^{-1}, \quad (17)$$

where  $\mathbf{R}_{\mathbf{m}\mathbf{d}} \equiv \langle \mathbf{m}\mathbf{d}^T \rangle$  and  $\mathbf{R}_{\mathbf{d}\mathbf{d}} \equiv \langle \mathbf{d}\mathbf{d}^T \rangle$  are model-data and data covariance matrices.

Since the data and models have been chosen, as shown in Eqs. (12) and (11), these matrices have the following block structure:

$$\mathbf{R}_{\mathbf{m}\mathbf{d}} = [\mathbf{B}_{\mathbf{m}\mathbf{d}}(t_0, t - N\tau), \mathbf{B}_{\mathbf{m}\mathbf{d}}(t_0, t - N\tau + \tau), \dots, \mathbf{B}_{\mathbf{m}\mathbf{d}}(t_0, t)], \quad (18)$$

$$\mathbf{R}_{\mathbf{d}\mathbf{d}} = \begin{bmatrix} \mathbf{B}_{\mathbf{d}\mathbf{d}}(t - N\tau, t - N\tau) & \mathbf{B}_{\mathbf{d}\mathbf{d}}(t - N\tau, t - N\tau + \tau) & \cdots & \mathbf{B}_{\mathbf{d}\mathbf{d}}(t - N\tau, t) \\ \mathbf{B}_{\mathbf{d}\mathbf{d}}(t - N\tau + \tau, t - N\tau) & \mathbf{B}_{\mathbf{d}\mathbf{d}}(t - N\tau + \tau, t - N\tau + \tau) & \cdots & \mathbf{B}_{\mathbf{d}\mathbf{d}}(t - N\tau + \tau, t) \\ \vdots & \vdots & \ddots & \vdots \\ \mathbf{B}_{\mathbf{d}\mathbf{d}}(t, t - N\tau) & \mathbf{B}_{\mathbf{d}\mathbf{d}}(t, t - N\tau + \tau) & \cdots & \mathbf{B}_{\mathbf{d}\mathbf{d}}(t, t) \end{bmatrix}. \quad (19)$$

Here  $\mathbf{B}_{\mathbf{m}\mathbf{d}}(t_1, t_2) \equiv \langle \mathbf{m}(t_1)\mathbf{d}^T(t_2) \rangle$  is the covariance matrix of size  $[3J, I]$  between the models at time moment  $t_1$  and data at moment  $t_2$ ,  $\mathbf{B}_{\mathbf{d}\mathbf{d}}(t_1, t_2) \equiv \langle \mathbf{d}(t_1)\mathbf{d}^T(t_2) \rangle$  is the covariance matrix of size  $[I, I]$  between data at moment  $t_1$  and data at moment  $t_2$ , and the comma between the elements of the  $\mathbf{R}_{\mathbf{m}\mathbf{d}}$  matrix denotes that the  $\mathbf{B}_{\mathbf{m}\mathbf{d}}$  matrices are arranged in a row. Thus, the dimensions of the  $\mathbf{R}_{\mathbf{m}\mathbf{d}}$  and  $\mathbf{R}_{\mathbf{d}\mathbf{d}}$  matrices are  $[3J, (N+1)I]$  and  $[(N+1)I, (N+1)I]$ , correspondingly. Note that the  $\mathbf{R}_{\mathbf{d}\mathbf{d}}$  matrix is symmetric.

It is assumed that noise in the data  $\xi(t)$  is independent of the sought fields and the noise-free data vectors, is not correlated with itself for different time moments and for different paths, and can be described by the normal distribution  $N(0, \sigma_\xi^2)$ . Therefore, in the presence of noise,

$$\mathbf{R}_{\mathbf{m}\mathbf{d}} = \mathbf{R}_{\mathbf{m}\mathbf{d}_0}, \quad (20)$$

$$\mathbf{R}_{\mathbf{d}\mathbf{d}} = \mathbf{R}_{\mathbf{d}_0\mathbf{d}_0} + \sigma_\xi^2 \mathbf{I}, \quad (21)$$

where  $\mathbf{I}$  is the identity matrix. Since noise in the data can easily be taken into account by these formulas, further considerations will be focused on the noise-free data  $\mathbf{d}_0$ .

It can be shown (see Appendix B) that the error covariance matrix  $\mathbf{R}_{\epsilon\epsilon}$  that corresponds to such an estimation of models [see Eq. (13)] with the optimal matrix  $\mathbf{A}$  given by Eq. (17) is

$$\mathbf{R}_{\epsilon\epsilon} = \mathbf{R}_{\mathbf{m}\mathbf{m}} - \mathbf{R}_{\mathbf{m}\mathbf{d}}\mathbf{R}_{\mathbf{d}\mathbf{d}}^{-1}\mathbf{R}_{\mathbf{d}\mathbf{m}}^T, \quad (22)$$

where  $\mathbf{R}_{\mathbf{m}\mathbf{m}} \equiv \langle \mathbf{m}(t_0)\mathbf{m}^T(t_0) \rangle$  is the models covariance matrix at time  $t_0$ . The elements of the main diagonal of the  $\mathbf{R}_{\epsilon\epsilon}$  matrix are equal to expected mean square errors of the reconstruction at each point. They can be calculated without knowledge of the original fields. These averaged errors can differ from the errors of the reconstruction of a particular realization of the original fields.

Note that the developed mathematical formalism of TDSI is valid for statistically nonstationary and inhomogeneous random fields.

### III. COVARIANCE MATRICES

Since the optimal stochastic inverse operator  $\mathbf{A}$  given by Eq. (17) is determined in terms of the  $\mathbf{R}_{\mathbf{m}\mathbf{d}}$  and  $\mathbf{R}_{\mathbf{d}\mathbf{d}}$  matrices, it is worthwhile to consider some important particular cases

$$\begin{aligned}
 [\mathbf{B}_{\mathbf{m}\mathbf{d}_0}(t_1, t_2)]_{ji} &= \langle m_j(t_1) d_{0i}(t_2) \rangle \\
 &= \int_{L_i} dl \left( \frac{c_0(t_2)}{2T_0(t_2)} \langle m_j(t_1) T(\mathbf{r}, t_2) \rangle + \langle m_j(t_1) u(\mathbf{r}, t_2) \rangle \cos \varphi_i + \langle m_j(t_1) v(\mathbf{r}, t_2) \rangle \sin \varphi_i \right) \\
 &= \begin{cases} \int_{L_i} dl \left( \frac{c_0(t_2)}{2T_0(t_2)} B_{TT}(\mathbf{r}_j, t_1; \mathbf{r}, t_2) \right), & \text{if } 1 \leq j \leq J, \\ \int_{L_i} dl (B_{uu}(\mathbf{r}_j, t_1; \mathbf{r}, t_2) \cos \varphi_i + B_{uv}(\mathbf{r}_j, t_1; \mathbf{r}, t_2) \sin \varphi_i), & \text{if } J+1 \leq j \leq 2J, \\ \int_{L_i} dl (B_{vu}(\mathbf{r}_j, t_1; \mathbf{r}, t_2) \cos \varphi_i + B_{vv}(\mathbf{r}_j, t_1; \mathbf{r}, t_2) \sin \varphi_i), & \text{if } 2J+1 \leq j \leq 3J, \end{cases} \quad (23)
 \end{aligned}$$

where  $i=1, 2, \dots, I$ ,  $j=1, 2, \dots, 3J$ ,  $\mathbf{r} \in L_i$ ,  $B_{TT}$ ,  $B_{uu}$ ,  $B_{vv}$ ,  $B_{uv}$ , and  $B_{vu}$  are the spatial-temporal covariance functions of the corresponding fields marked as the subscripts, and the  $\mathbf{r}_j$  are the chosen spatial points within the tomographic area at which the sought fields are reconstructed; these points stay fixed during the integration.

Similarly, an expression for the covariance matrix  $\mathbf{B}_{d_0 d_0}(t_1, t_2)$  between the noise-free data at time  $t_1$  and time  $t_2$  is given by

$$\begin{aligned}
 [\mathbf{B}_{d_0 d_0}(t_1, t_2)]_{ip} &= \langle d_{0i}(t_1) d_{0p}(t_2) \rangle = \int_{L_i} dl \int_{L_p} dl' \left\{ \frac{c_0(t_1) c_0(t_2)}{4T_0(t_1) T_0(t_2)} B_{TT}(\mathbf{r}, t_1; \mathbf{r}', t_2) + B_{uu}(\mathbf{r}, t_1; \mathbf{r}', t_2) \cos \varphi_i \cos \varphi_p \right. \\
 &\quad \left. + B_{vv}(\mathbf{r}, t_1; \mathbf{r}', t_2) \sin \varphi_i \sin \varphi_p + B_{uv}(\mathbf{r}, t_1; \mathbf{r}', t_2) \cos \varphi_i \sin \varphi_p + B_{vu}(\mathbf{r}, t_1; \mathbf{r}', t_2) \sin \varphi_i \cos \varphi_p \right\}, \quad (24)
 \end{aligned}$$

where  $i, p=1, 2, \dots, I$ ,  $\mathbf{r} \in L_i$ ,  $\mathbf{r}' \in L_p$ . Note that  $B_{vu}(\mathbf{r}, t_1; \mathbf{r}', t_2) = B_{uv}(\mathbf{r}', t_2; \mathbf{r}, t_1)$ . When deriving Eqs. (23) and (24), it is assumed that  $B_{Tu} = B_{Tv} = 0$ .

Once the matrices  $\mathbf{B}_{\mathbf{m}\mathbf{d}_0}(t_1, t_2)$  and  $\mathbf{B}_{d_0 d_0}(t_1, t_2)$  are calculated, one should use Eqs. (18) and (19) to form the  $\mathbf{R}_{\mathbf{m}\mathbf{d}_0}$  and  $\mathbf{R}_{d_0 d_0}$  matrices and, then, Eq. (21) to take noise into account.

### B. Stationary fields

If the temperature and wind velocity fields are statistically stationary, their covariance functions depend only on the difference of their temporal arguments:

$$B(\mathbf{r}, t_1; \mathbf{r}', t_2) = B(\mathbf{r}, \mathbf{r}', \Delta t), \quad \Delta t \equiv t_2 - t_1. \quad (25)$$

The notation  $B$  without subscripts stands for the covariance function of any two fields considered above. In this case, Eqs. (18) and (19) are modified as follows:

when these matrices can be calculated explicitly. These considerations will be carried out taking 2-D travel-time tomography of the atmosphere as an example.

### A. 2-D travel-time tomography

In the case of travel-time tomography, one can use the linear relationship between  $\mathbf{d}_0$  and the sought fields given by Eq. (10) to obtain an expression for the covariance matrix  $\mathbf{B}_{\mathbf{m}\mathbf{d}_0}(t_1, t_2)$  between the models at time  $t_1$  and the noise-free data at time  $t_2$ :

$$\begin{aligned}
 \mathbf{R}_{\mathbf{m}\mathbf{d}} &= [\mathbf{B}_{\mathbf{m}\mathbf{d}}(t - N\tau - t_0), \mathbf{B}_{\mathbf{m}\mathbf{d}}(t - N\tau + \tau - t_0), \dots, \\
 &\quad \mathbf{B}_{\mathbf{m}\mathbf{d}}(t - t_0)], \quad (26)
 \end{aligned}$$

$$\mathbf{R}_{\mathbf{d}\mathbf{d}} = \begin{bmatrix} \mathbf{B}_{dd}(0) & \mathbf{B}_{dd}(\tau) & \cdots & \mathbf{B}_{dd}(N\tau) \\ \mathbf{B}_{dd}(-\tau) & \mathbf{B}_{dd}(0) & \cdots & \mathbf{B}_{dd}(N\tau - \tau) \\ \vdots & \vdots & \ddots & \vdots \\ \mathbf{B}_{dd}(-N\tau) & \mathbf{B}_{dd}(-N\tau + \tau) & \cdots & \mathbf{B}_{dd}(0) \end{bmatrix}. \quad (27)$$

Note that, for any  $\Delta t$ ,

$$\mathbf{B}_{dd}(\Delta t) = \mathbf{B}_{dd}^T(-\Delta t). \quad (28)$$

It is sufficient to know only the first cell row of the matrix  $\mathbf{R}_{\mathbf{d}\mathbf{d}}$  since it has the same matrices along each diagonal (a block Toeplitz-like structure). Also note that the  $\mathbf{R}_{\mathbf{d}\mathbf{d}}$  matrix is independent of time  $t_0$ , i.e., for the given set of data it is

necessary to calculate this matrix only once to reconstruct fields at any time. Another interesting fact is that the matrices  $\mathbf{B}_{dd}(0)$  on its main diagonal are equal to the covariance matrix  $\mathbf{R}_{dd}$  of ordinary SI.

### C. Frozen turbulence

If turbulence may be considered frozen, each spatial point of the temperature and wind velocity fields is moving with a constant speed  $\mathbf{U}$ . In this case, the temperature field at time  $t_2$  can be expressed in terms of the field at time  $t_1$  by the following relationship:<sup>20</sup>

$$T(\mathbf{r}, t_2) = T(\mathbf{r} - \mathbf{U} \Delta t, t_1). \quad (29)$$

The same relationship is valid for the turbulent wind velocity fields. This allows one to obtain the spatial-temporal covariance matrices, which are unknown in general, in terms of the spatial covariance matrices. The latter can be modeled by the covariance functions corresponding, for example, to the von Kármán or Gaussian spatial spectra of turbulence. For example, for the temperature field, we have

$$\begin{aligned} B_{TT}(\mathbf{r}, t_1; \mathbf{r}', t_2) &\equiv \langle T(\mathbf{r}, t_1) T(\mathbf{r}', t_2) \rangle \\ &= \langle T(\mathbf{r}, t_1) T(\mathbf{r}' - \mathbf{U} \Delta t, t_1) \rangle = B_{TT}^s(\mathbf{r}, \mathbf{r}' - \mathbf{U} \Delta t), \end{aligned} \quad (30)$$

where  $B_{TT}^s$  is the spatial covariance matrix of the temperature field. The last equality is true for statistically stationary fields. Similar equations can be derived for the spatial-temporal covariance functions of the other fields. Since frozen turbulence is a particular case of stationary fields, Eqs. (26)–(28), stay valid for this case as well. Thus, for frozen turbulence the spatial-temporal covariance matrices  $\mathbf{R}_{md}$  and  $\mathbf{R}_{dd}$  can be expressed in terms of known or inferred spatial covariance matrices.

The frozen turbulence hypothesis is widely used in meteorology and the study of wave propagation in random media, e.g., Refs. 20 and 21. This hypothesis is valid with a good accuracy for eddies in the inertial range of turbulence. However, the applicability of this hypothesis to eddies in the energy range is questionable.<sup>22</sup> Note that in the present paper, the frozen turbulence hypothesis is used to concretize the spatial-temporal covariance functions. TDSI can still be used if this hypothesis is invalid.

### IV. NUMERICAL EXPERIMENT

In this section, a numerical experiment that demonstrates the significant improvement in the quality of temperature and wind velocity field reconstructions possible with TDSI is described. A snapshot of the temperature and wind velocity fields was created by large eddy simulation (LES),<sup>23</sup> which is widely used in meteorology (e.g., Refs. 24 and 25). LES numerically solves the Navier-Stokes equations for eddies large enough to be resolved by the spatial grid. The effect of smaller eddies on the resolved flow is parametrized. LES produces realistic wind velocity and temperature fields for flow processes that are well resolved by the grid.

Using the single snapshot of the LES temperature and wind velocity fields, the perfectly frozen turbulent fields with

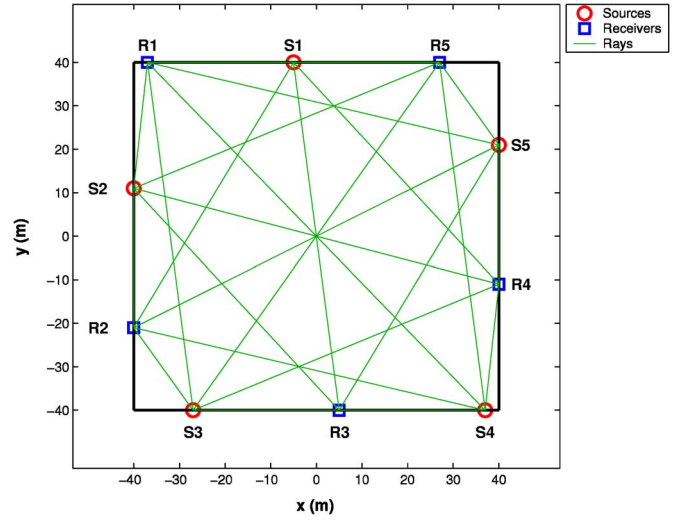


FIG. 1. (Color online) The layout of sources and receivers in the numerical experiment.

the velocity components  $U_x=4$  m/s and  $U_y=0$  m/s were created. The travel times were calculated each second ( $\tau=1$  s) using Eq. (5). Two-dimensional linear interpolation was employed to obtain the value of the integrand in Eq. (5) along the travel paths; then the integral was calculated numerically. These travel times were disturbed by white noise with standard deviation  $\sigma_\varepsilon=5$   $\mu$ s, which corresponds to relative errors of order 1% to 42% in the data  $d_0(t)$ . The total number of such numerical scans was 18, and the problem was to estimate the temperature and wind velocity fields  $T_{av}(\mathbf{r}, t_0)$ ,  $\bar{u}(\mathbf{r}, t_0)$ , and  $\bar{v}(\mathbf{r}, t_0)$  at time  $t_0=9$  s. The time origin coincided with the first scan. The number of sources as well as receivers was 5, so that the number of rays  $l$  at each scan was 25. The tomographic area was a square of 80 by 80 meters. The layout of acoustic sources and receivers and the corresponding ray paths are shown in Fig. 1.

The reconstruction consisted of two stages. In the first stage the spatial mean values of the temperature and wind velocity fields  $T_0(t_0)$ ,  $u_0(t_0)$ , and  $v_0(t_0)$  within the tomographic area were reconstructed using the approach described in Sec. II B. The true and estimated spatial mean values of temperature and wind fields are presented in Table I.

One can see from Table I that the reconstruction of spatial mean fields was very accurate, the differences between true and estimated mean values was 0.14 K for the temperature field, 0.03 m/s for the  $x$  component of the wind velocity vector, and 0.01 m/s for its  $y$  component.

In the second stage, the fluctuations of the temperature and wind fields  $T(\mathbf{r}, t_0)$ ,  $u(\mathbf{r}, t_0)$ , and  $v(\mathbf{r}, t_0)$  from their spatial mean values were reconstructed using either standard SI (only data at time  $t_0$  were used, the total number of data

TABLE I. Actual and estimated spatial mean values of temperature and wind velocity fields.

Mean fields	$T_0$ (K)	$u_0$ (m/s)	$v_0$ (m/s)
True	301.73	3.09	1.73
Estimated	301.87	3.06	1.71

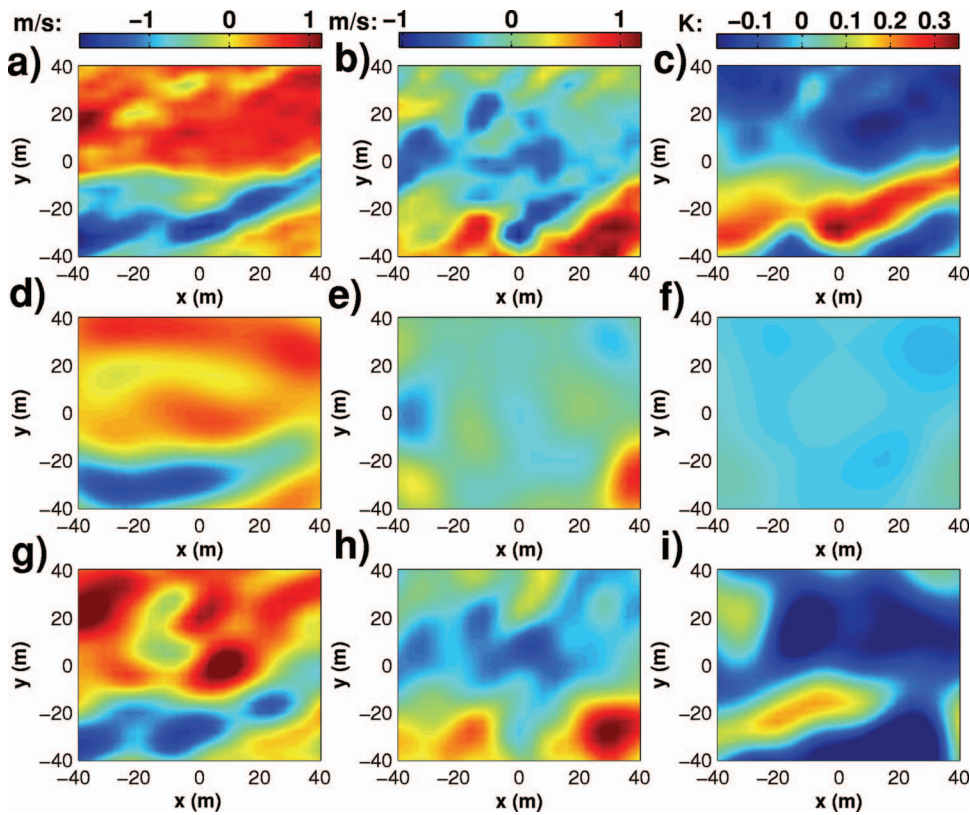


FIG. 2. The original and reconstructed temperature (K) and wind velocity (m/s) fields of fluctuations at time moment  $t_0=9$  s. (a) Original  $u$  field. (b) Original  $v$  field. (c) Original  $T$  field. (d) The  $u$  field reconstructed by SI. (e) The  $v$  field reconstructed by SI. (f) The  $T$  field reconstructed by SI. (g) The  $u$  field reconstructed by TDSI. (h) The  $v$  field reconstructed by TDSI. (i) The  $T$  field reconstructed by TDSI.

points was equal to the number of rays  $I=25$ ) or TDSI (data obtained at 18 different times were used, which resulted in 450 data points). To describe the spatial covariance of the temperature and wind velocity fields within the tomographic area, the following Gaussian covariance functions were used:<sup>11</sup>

$$B_{TT}^s(\mathbf{r}, \mathbf{r}') = \sigma_T^2 \exp\left(-\frac{(\mathbf{r} - \mathbf{r}')^2}{l_T^2}\right), \quad (31)$$

$$B_{uu}^s(\mathbf{r}, \mathbf{r}') = \sigma_u^2 \exp\left(-\frac{(\mathbf{r} - \mathbf{r}')^2}{l^2}\right) \left(1 - \frac{(y - y')^2}{l^2}\right), \quad (32)$$

$$B_{vv}^s(\mathbf{r}, \mathbf{r}') = \sigma_v^2 \exp\left(-\frac{(\mathbf{r} - \mathbf{r}')^2}{l^2}\right) \left(1 - \frac{(x - x')^2}{l^2}\right), \quad (33)$$

$$B_{uv}^s(\mathbf{r}, \mathbf{r}') = \sigma_u \sigma_v \exp\left(-\frac{(\mathbf{r} - \mathbf{r}')^2}{l^2}\right) \frac{(x - x')(y - y')}{l^2}, \quad (34)$$

where  $\sigma_T, \sigma_u, \sigma_v$  are the standard deviations of the corresponding fields,  $l_T$  and  $l$  are their correlation lengths,  $\mathbf{r} = (x, y)$ , and  $\mathbf{r}' = (x', y')$ . Then, the relations similar to that given by Eq. (30) were used to obtain the spatial-temporal covariance functions of the sought fields. The noise-free matrices  $\mathbf{R}_{\text{md}_0}$  and  $\mathbf{R}_{\text{d}_0\text{d}_0}$  were formed with the help of Eqs. (26) and (27), where the  $\mathbf{B}_{\text{md}_0}$  and  $\mathbf{B}_{\text{d}_0\text{d}_0}$  matrices were calculated using Eqs. (23) and (24); noise was taken into account by Eq. (21).

In the described numerical experiment, there were five parameters in the SI and TDSI algorithms that must be cho-

sen:  $\sigma_T, \sigma_u, \sigma_v, l_T$ , and  $l$ . These parameters were estimated from the original LES fields:  $\sigma_T=0.14$  K,  $\sigma_u=0.72$  m/s,  $\sigma_v=0.42$  m/s, and  $l_T=l=15$  m.

The original and reconstructed fields were described by matrices of size 21 by 21. After all calculations were done, the fields were interpolated (2-D linear interpolation) for illustrative purposes. The fluctuating parts of the original fields are presented in Figs. 2(a)–2(c). Figures 2(d)–2(f) show the reconstructed fields using the SI approach. The reconstruction results of TDSI are given in Figs. 2(g)–2(i). As one can see, standard SI matched the contours of the sought  $u$  field fairly well, but the  $v$  and  $T$  fields were reconstructed poorly. In contrast, the time-dependent stochastic approach allowed the much more detailed and accurate reconstruction of all fields. To characterize the expected improvement of the reconstruction it is worthwhile to consider the expected errors of the reconstruction given by Eq. (22). It is convenient to normalize these mean square errors by the corresponding field variances so that their values lie in  $[0, 1]$ . If these normalized mean-squared errors (NMSE) are of order unity, the errors of reconstruction are of the order of variance of the original field, i.e., one has a poor reconstruction. Conversely, if NMSE are zeros, it is expected that the reconstructed and actual fields are identical. NMSE can be recalculated into root mean-square errors (RMSE). NMSE for SI are presented in Figs. 3(a)–3(c) while Figs. 3(d)–3(f) show NMSE for TDSI. To characterize the overall quality of the reconstruction, NMSE at each spatial point and corresponding RMSE were averaged over the tomographic area. These averaged values of NMSE and RMSE are presented in Table II.

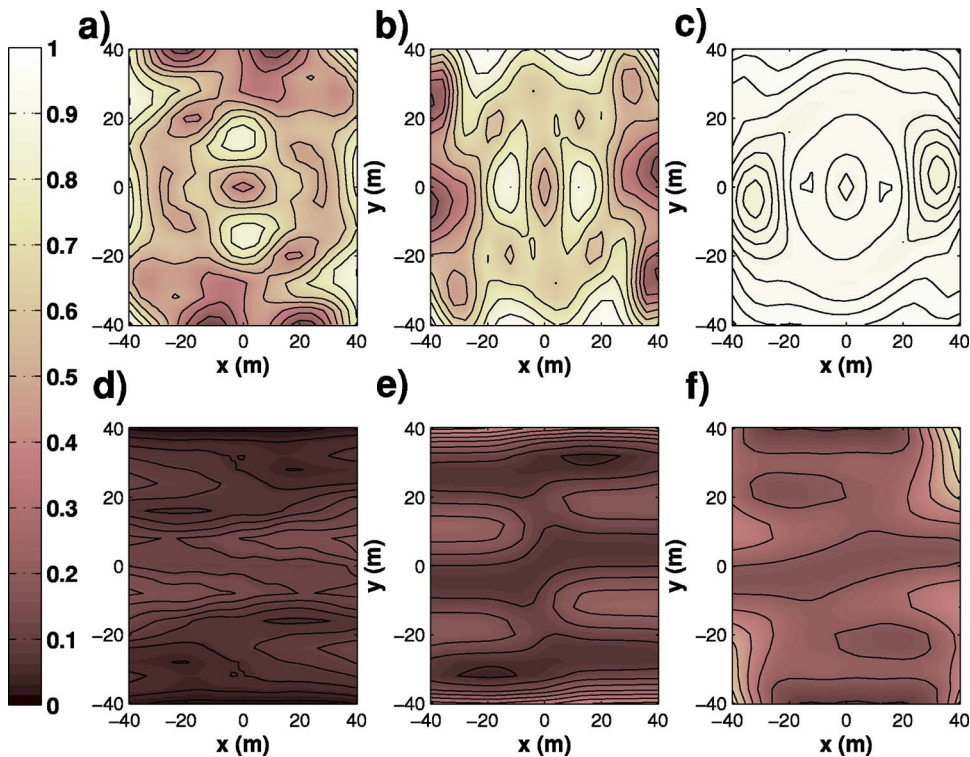


FIG. 3. (Color online) The expected normalized mean square errors. (a) The  $u$  field reconstructed by SI. (b) The  $v$  field reconstructed by SI. (c) The  $T$  field reconstructed by SI. (d) The  $u$  field reconstructed by TDSI. (e) The  $v$  field reconstructed by TDSI. (f) The  $T$  field reconstructed by TDSI.

It follows from Fig. 3 and Table II that, for TDSI, the average NMSE is about four times less for the  $T$  and  $v$  fields and seven times less for the  $u$  field than the corresponding NMSE for ordinary SI. This corresponds to a 46% reduction of the RMSE for the  $T$  field, a 52% reduction for the  $v$  fields, and a 62% reduction for the  $u$  field.

## V. DISCUSSION

The idea of the stochastic approach is based on the assumption that covariance matrices of the sought fields are known. That means that in the case of the Gaussian covariance functions all five parameters (variances and correlation lengths of the sought fields) should be known in advance. In the practical implementation of travel-time tomography, however, these parameters are unknown. One can estimate these parameters by measuring the temperature and wind velocity fluctuations with the use of conventional meteorological sensors or using a turbulence similarity theory.

Furthermore, the covariance of the isotropic turbulence in the atmosphere is better described by the von Kármán spectrum rather than by the Gaussian spectrum. The latter was used in the numerical experiment because it was then possible to calculate the  $\mathbf{R}_{md}$  matrix analytically and use only a single numeric integration to get the  $\mathbf{R}_{dd}$  matrix. This

significantly improved the accuracy and speed of the calculations. Since the actual fields were not described by the Gaussian covariance functions, the reconstruction quality improvement seems rather unexpected. However, there is a relatively simple explanation of this fact. In a certain spatial scale range, the covariance functions of atmospheric turbulence can be approximated by the Gaussian covariance functions with appropriate variances and correlation lengths.<sup>27</sup> Therefore, the Gaussian covariance functions can be used for SI and TDSI as approximations of the actual ones. It is expected that the use of the covariance function corresponding to the von Kármán spectrum of turbulence will improve the reconstruction.

One of the advantages of the stochastic approach is that noise in the data plays, in a certain sense, a positive role by regularizing the  $\mathbf{R}_{dd}$  matrix [see Eq. (21)]. Indeed, the presence of noise just adds an additional term to the main diagonal of the  $\mathbf{R}_{dd}$  matrix, which improves its condition (keeps it invertible), although it does smooth the solution somewhat. This regularization is especially important for TDSI, where the condition of the matrix  $\mathbf{R}_{dd}$  may be very poor and may lead to spurious solutions.

Figures 2(a)–2(i) show that the reconstruction of the temperature fluctuation field was not as good as that for the velocity fluctuations. The probable reason for this is a small effect of the temperature fluctuations on the travel times in comparison to the wind-velocity fluctuations. Indeed, the LES temperature fluctuations were in the range  $[-0.15, 0.35]$  K while, for many meteorological problems, the acceptable error of temperature measurements is  $\pm 0.3$  K.<sup>7,8</sup> Note that to improve the reconstruction of temperature fluctuations in acoustic tomography, one can use reciprocal transmission of sound waves.<sup>8,26</sup>

TABLE II. Average expected errors of the reconstruction of temperature and wind velocity fields by SI and TDSI.

Fields	$T$		$u$		$v$	
Errors	NMSE	RMSE (K)	NMSE	RMSE (m/s)	NMSE	RMSE (m/s)
SI	0.96	0.13	0.56	0.53	0.63	0.33
TDSI	0.24	0.07	0.08	0.20	0.15	0.16

The proposed TDSI algorithm also allows one to estimate the temporal mean values of the temperature and wind velocity fluctuations at any given spatial point. This might be important when the temporal changes of these fluctuations are negligible during the time interval  $N\tau$ . For this purpose, it is necessary to set all temporal arguments in the matrices  $\mathbf{R}_{\text{md}}$  and  $\mathbf{R}_{\text{dd}}$  equal to zero. Note that in this case the noise variance  $\sigma_\xi^2$  should be enlarged, because the noise includes not only the measurement uncertainty but also the neglected variation of the original fields during the observed time interval.

## VI. CONCLUSION

In this paper, a generalization of the stochastic inversion approach for tomographic problems in the atmosphere was developed. The key idea of this generalization is that, by using spatial-temporal covariance functions of temperature and wind velocity fields, one can use data obtained at different times to reconstruct these fields at any particular time. This allows one to significantly enlarge the effective amount of tomographic data, while keeping the total number of sources and/or receivers fixed. The efficiency of the developed method was demonstrated in a numerical experiment that simulated the acoustic 2-D travel-time tomography problem of the atmosphere. This numerical experiment showed a remarkable improvement of the reconstruction when one used TDSI instead of standard SI.

## ACKNOWLEDGMENTS

This material is partly based upon work that was supported by the U.S. Army Research Office under Contracts No. DAAD19-03-1-0104 and No. DAAD19-03-1-0341. Also, we would like to thank E. G. Patton and P. P. Sullivan of the National Center for Atmospheric Research for providing the LES data. The LES was supported in part by the DoD High-Performance Computing Modernization Program. Finally, we would like to thank anonymous reviewers, whose comments allowed us to improve this paper.

## APPENDIX A: OPTIMAL STOCHASTIC OPERATOR DERIVATION

Let  $\mathbf{m}$  and  $\mathbf{d}$  be two arbitrary random column-vectors of lengths  $M$  and  $D$ , correspondingly, with a known matrix of the second statistical moment  $\mathbf{R}_{\text{md}} \equiv \langle \mathbf{m}\mathbf{d}^T \rangle$ . Furthermore, let the matrix  $\mathbf{R}_{\text{dd}} \equiv \langle \mathbf{d}\mathbf{d}^T \rangle$  also be known. Note that, in the case when  $\langle \mathbf{m} \rangle = \mathbf{0}$ ,  $\langle \mathbf{d} \rangle = \mathbf{0}$ , the  $\mathbf{R}_{\text{md}}$  and  $\mathbf{R}_{\text{dd}}$  are the covariance matrices. The problem is to estimate the unknown vector  $\mathbf{m}$  if a particular realization of the random vector  $\mathbf{d}$  is given. To do this, one can seek for the estimation  $\hat{\mathbf{m}}$  of the unknown vector  $\mathbf{m}$  in the form

$$\hat{\mathbf{m}} = \mathbf{A}\mathbf{d}. \quad (\text{A1})$$

Introduce the column vector of discrepancy  $\boldsymbol{\epsilon}$  between the true and reconstructed vectors:

$$\epsilon_j = \hat{m}_j - m_j, \quad (\text{A2})$$

where  $j = 1, 2, \dots, M$ .

To find the elements  $a_{jk}$  of matrix  $\mathbf{A}$ , let us require that they give the minimum of each element of the mean square errors vector  $\langle \boldsymbol{\epsilon}^2 \rangle$ :

$$\langle \epsilon_j^2 \rangle \mapsto \min_{\{a_{jk}\}} \langle \epsilon_j^2 \rangle, \quad (\text{A3})$$

where  $k = 1, 2, \dots, D$ .

To satisfy the requirement (A3), one should take the partial derivative along the current element  $a_{ip}$  of the matrix  $\mathbf{A}$  and make it equal to 0:

$$\begin{aligned} \frac{\partial}{\partial a_{ip}} \langle (a_{jk}d_k - m_j)^2 \rangle &= 2 \langle (a_{ik}d_k - m_i)d_p \rangle \\ &= 2(a_{ik} \langle d_k d_p \rangle - \langle m_i d_p \rangle) \\ &= 2(a_{ik} [\mathbf{R}_{\text{dd}}]_{kp} - [\mathbf{R}_{\text{md}}]_{ip}) = 0, \end{aligned} \quad (\text{A4})$$

where the equality  $\partial a_{jk} / \partial a_{ip} \equiv \delta_{ij} \delta_{pk}$  was taken into account, and the  $\delta$ 's are Kronecker's delta symbols. The last equation, after canceling the factor 2, can be written in matrix notation:

$$\mathbf{A}\mathbf{R}_{\text{dd}} - \mathbf{R}_{\text{md}} = \mathbf{0}. \quad (\text{A5})$$

Therefore, under assumption that the inverse matrix  $\mathbf{R}_{\text{dd}}^{-1}$  exists, the optimal matrix  $\mathbf{A}$  is given by

$$\mathbf{A} = \mathbf{R}_{\text{md}}\mathbf{R}_{\text{dd}}^{-1}. \quad (\text{A6})$$

## APPENDIX B: ERROR COVARIANCE MATRIX DERIVATION

If a random column vector  $\boldsymbol{\eta}$  relates to another random column vector  $\boldsymbol{\xi}$  by a known nonrandom matrix  $\mathbf{C}$  as  $\boldsymbol{\eta} = \mathbf{C}\boldsymbol{\xi}$ , then its covariance matrix  $\mathbf{R}_{\boldsymbol{\eta}\boldsymbol{\eta}} \equiv \langle \boldsymbol{\eta}\boldsymbol{\eta}^T \rangle$  is expressed in terms of the covariance matrix  $\mathbf{R}_{\boldsymbol{\xi}\boldsymbol{\xi}} \equiv \langle \boldsymbol{\xi}\boldsymbol{\xi}^T \rangle$  as

$$\mathbf{R}_{\boldsymbol{\eta}\boldsymbol{\eta}} = \mathbf{C}\mathbf{R}_{\boldsymbol{\xi}\boldsymbol{\xi}}\mathbf{C}^T. \quad (\text{B1})$$

In the case of travel-time tomography, the column vector of discrepancy is given by  $\boldsymbol{\epsilon} \equiv \hat{\mathbf{m}} - \mathbf{m}$ , where  $\hat{\mathbf{m}} = \mathbf{A}\mathbf{d}$ . Therefore, the discrepancy can be expressed in terms of the matrix multiplication using block matrix notation:

$$\boldsymbol{\epsilon} = [\mathbf{A} - \mathbf{I}] \begin{bmatrix} \mathbf{d} \\ \mathbf{m} \end{bmatrix}, \quad (\text{B2})$$

where  $\mathbf{I}$  is the identical matrix. Using the formula (B1), one can get the expression for covariance matrix  $\mathbf{R}_{\boldsymbol{\epsilon}\boldsymbol{\epsilon}}$ :

$$\begin{aligned} \mathbf{R}_{\boldsymbol{\epsilon}\boldsymbol{\epsilon}} &= [\mathbf{A} - \mathbf{I}] \left\langle \begin{bmatrix} \mathbf{d} \\ \mathbf{m} \end{bmatrix} \begin{bmatrix} \mathbf{d}^T \mathbf{m}^T \end{bmatrix} \right\rangle \begin{bmatrix} \mathbf{A}^T \\ -\mathbf{I} \end{bmatrix} \\ &= [\mathbf{A} - \mathbf{I}] \begin{bmatrix} \langle \mathbf{d}\mathbf{d}^T \rangle & \langle \mathbf{d}\mathbf{m}^T \rangle \\ \langle \mathbf{m}\mathbf{d}^T \rangle & \langle \mathbf{m}\mathbf{m}^T \rangle \end{bmatrix} \begin{bmatrix} \mathbf{A}^T \\ -\mathbf{I} \end{bmatrix} \\ &= \mathbf{A}\mathbf{R}_{\text{dd}}\mathbf{A}^T - \mathbf{A}\mathbf{R}_{\text{md}}^T - \mathbf{R}_{\text{md}}\mathbf{A}^T + \mathbf{R}_{\text{mm}}. \end{aligned} \quad (\text{B3})$$

Note that this formula for the covariance matrix of the discrepancy vector is valid for any matrix  $\mathbf{A}$ . Since the optimal matrix  $\mathbf{A}$  of the stochastic inversion and time-dependent stochastic inversion is given by  $\mathbf{A} = \mathbf{R}_{\text{md}}\mathbf{R}_{\text{dd}}^{-1}$ , the  $\mathbf{R}_{\boldsymbol{\epsilon}\boldsymbol{\epsilon}}$  matrix takes the form

$$\mathbf{R}_{\epsilon\epsilon} = \mathbf{R}_{mm} - \mathbf{R}_{md}\mathbf{R}_{dd}^{-1}\mathbf{R}_{md}^T \quad (\text{B4})$$

Note that the diagonal elements of the error covariance matrix  $\mathbf{R}_{\epsilon\epsilon}$  represent the mean square errors of the estimation  $\hat{\mathbf{m}}$ .

- <sup>1</sup>D. K. Wilson, A. Ziemann, V. E. Ostashev, and A. G. Voronovich, "An overview of acoustic travel-time tomography in the atmosphere and its potential applications," *Acta. Acust. Acust.* **87**, 721–730 (2001).
- <sup>2</sup>S. N. Vecherin, V. E. Ostashev, D. K. Wilson, A. G. Voronovich, G. H. Goedecke, S. L. Collier, J. M. Noble, and D. Ligon, "Forward and inverse problems of acoustic tomography of the atmosphere," *Proc. 11th Intern. Symp. on Long Range Sound Propagation*, Fairlee, VT, 2004.
- <sup>3</sup>D. K. Wilson, V. E. Ostashev, S. N. Vecherin, A. G. Voronovich, S. L. Collier, and J. M. Noble, "Assessment of acoustic travel-time tomography of the atmospheric surface layer," *Proceedings of AMS Symposium on Boundary Layers and Turbulence*, Portland, ME, 2004.
- <sup>4</sup>S. L. Collier, D. A. Ligon, J. M. Noble, E. Patton, P. Sullivan, and V. E. Ostashev, "Acoustic tomographic array simulation," *Proc. 11th Intern. Symp. on Long Range Sound Propagation*, Fairlee, VT, 2004.
- <sup>5</sup>D. K. Wilson and D. W. Thomson, "Acoustic tomographic monitoring of the atmospheric surface layer," *J. Atmos. Ocean. Technol.* **11**, 751–769 (1994).
- <sup>6</sup>K. Arnold, A. Ziemann, and A. Raabe, "Acoustic tomography inside the atmospheric boundary layer," *Phys. Chem. Earth, Part B* **24**, 133–137 (1999).
- <sup>7</sup>A. Ziemann, K. Arnold, and A. Raabe, "Acoustic tomography in the atmospheric surface layer," *Ann. Geophys.* **17**, 139–148 (1999).
- <sup>8</sup>A. Ziemann, K. Arnold, and A. Raabe, "Acoustic travel-time tomography—a method for remote sensing of the atmospheric surface layer," *Meteorol. Atmos. Phys.* **71**, 43–51 (1999).
- <sup>9</sup>A. Ziemann, K. Arnold, and A. Raabe, "Acoustic tomography as a method to identify small-scale land surface characteristics," *Acta. Acust. Acust.* **87**, 731–737 (2001).
- <sup>10</sup>K. Arnold, A. Ziemann, and A. Raabe, "Tomographic monitoring of wind and temperature at different heights above the ground," *Acta. Acust. Acust.* **87**, 703–708 (2001).
- <sup>11</sup>V. E. Ostashev, *Acoustics in Moving Inhomogeneous Media* (E&FN SPON, London, 1997).
- <sup>12</sup>P. Holstein, A. Raabe, R. Müller, M. Barth, D. Mackenzie, and E. Starke, "Acoustic tomography on the basis of travel-time measurement," *Meas. Sci. Technol.* **15**, 1420–1428 (2004).
- <sup>13</sup>M. Barth, A. Raabe, P. Holstein, R. Muller, A. Ziemann, K. Arnold, D. Mackenzie, E. Starke, and M. Seliger, "Acoustic travel-time tomography as a tool to investigate temperature distributions on different spatial scales," *12th International Symposium on Acoustic Remote Sensing and Associated Techniques of the Atmosphere and Oceans*, Cambridge, UK, 2004.
- <sup>14</sup>K. Aki and P. G. Richards, *Quantitative Seismology. Theory and Methods* (Freeman, San Francisco, 1980).
- <sup>15</sup>V. E. Ostashev, B. Brähler, V. Mellert, and G. H. Goedecke, "Coherence functions of plane and spherical waves in a turbulent medium with the von Kármán spectrum of medium inhomogeneities," *J. Acoust. Soc. Am.* **104**, 727–737 (1998).
- <sup>16</sup>V. E. Ostashev, V. Mellert, R. Wandelt, and F. Gerdes, "Propagation of sound in a turbulent medium I. Plane waves," *J. Acoust. Soc. Am.* **102**, 2561–2570 (1997).
- <sup>17</sup>J. Gilson, D. Roemmich, B. D. Cornuelle, and L.-L. Fu, "Relationship of TOPEX/Poseidon altimetric height to steric height and circulation in the North Pacific," *J. Geophys. Res.* **103**, 965 (1998).
- <sup>18</sup>N. Ducet, P. Y. Le Traon, and G. Reverdin, "Global high-resolution mapping of ocean circulation from TOPEX/Poseidon and ERS-1 and -2," *J. Geophys. Res.* **105**, 498 (2000).
- <sup>19</sup>F. P. Bretherton, R. E. Davis, and C. B. Fandry, "A technique for objective analysis and design of oceanographic experiments applied to MODE-73," *Deep-Sea Res.* **23**, 559–582 (1976).
- <sup>20</sup>J. Hinze, *Turbulence* (McGraw-Hill, New York, 1975).
- <sup>21</sup>V. I. Tatarskii, *The Effects of the Turbulent Atmosphere on Wave Propagation* (Keter, Jerusalem, 1971).
- <sup>22</sup>J. C. Kaimal and J. J. Finnigan, *Atmospheric Boundary Layer Flows: Their Structure and Measurement* (Oxford University Press, New York, 1994).
- <sup>23</sup>V. E. Ostashev, S. N. Vecherin, G. H. Goedecke, D. K. Wilson, A. G. Voronovich, and E. G. Patton, "Numerical simulation of acoustic tomography of the atmosphere," *J. Acoust. Soc. Am.* **117**, 2532 (2005).
- <sup>24</sup>A. Andren, A. R. Brown, J. Graf, P. J. Mason, C. H. Moeng, F. T. M. Nieuwstadt, and U. Schumann, "Large-eddy simulation of a neutrally stratified boundary layer: A comparison of four computer codes," *Q. J. R. Meteorol. Soc.* **120**, 1457–1484 (1994).
- <sup>25</sup>R. B. Stull, *An Introduction to Boundary Layer Meteorology* (Kluwer, Dordrecht, 1988).
- <sup>26</sup>W. H. Munk, P. Worcester, and C. Wunsch, *Ocean Acoustic Tomography* (Cambridge University Press, New York, 1995).
- <sup>27</sup>D. K. Wilson, J. G. Brasseur, and K. E. Gilbert, "Acoustic scattering and the spectrum of atmospheric turbulence," *J. Acoust. Soc. Am.* **105**, 30–34 (1999).